



Green and highly efficient approach for the reductive coupling of nitroarenes to azoxyarenes using the new mesoporous $\text{Fe}_3\text{O}_4@\text{SiO}_2@\text{Co-Zr-Sb}$ catalyst

Behzad Zeynizadeh¹ · Masumeh Gilanizadeh¹

Received: 18 December 2019 / Accepted: 10 March 2020
© Springer Nature B.V. 2020

Abstract

Efficient, green, simple and environmentally friendly approach for the straightforward reductive coupling of nitroarenes to the corresponding azoxyarenes has been developed in the presence of $\text{Fe}_3\text{O}_4@\text{SiO}_2@\text{Co-Zr-Sb}$ as a novel recyclable nanocatalyst. The Co-Zr-Sb trimetallic nanoparticles immobilized on silica-layered magnetite have been prepared by the co-precipitation method. The mesoporous catalyst has been characterized by FT-IR, SEM, EDX, VSM, TEM and XRD analyses. The chemoselective hydrogenation of nitrobenzenes was carried out successfully in refluxing water to afford the corresponding azoxybenzenes within 2–10 min in good to high yields. The reusability of the heterogeneous nanocatalyst has also been studied using the FT-IR and SEM analyses. The catalyst was utilized four times in sequential runs without significant loss of activity. The current research includes remarkable advantages of short reaction times, absence of hazardous organic solvents, mild reaction conditions, high yields, using water as a green solvent and the ability to utilize the recyclable nanomagnetic catalyst.

Keywords $\text{Fe}_3\text{O}_4@\text{SiO}_2@\text{Co-Zr-Sb}$ · Azoxybenzenes · Nanocatalyst · Nitroarenes · Reductive coupling

Introduction

Azoxybenzenes or diphenyldiazeno oxides have been considered as one of the important and prominent intermediates in material science, pharmaceuticals and agrochemicals [1]. These materials, as 1,3-dipolar compounds, are composed of an unusual oxygen–nitrogen–nitrogen bond in their structure [2]. Azoxyarenes have been utilized as polymerization inhibitors, therapeutic medicines, chemical

✉ Masumeh Gilanizadeh
masumehgilanizadeh@gmail.com

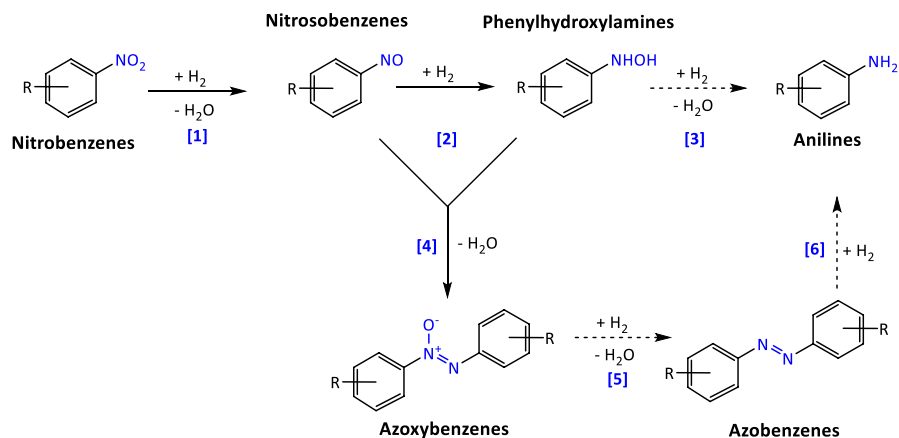
¹ Faculty of Chemistry, Urmia University, Urmia 5756151818, Iran

stabilizers, reducing agents, dyes, analytical reagents and also key building blocks for electronic devices [3–8]. Commonly, these types of compounds are prepared by the oxidation of anilines and reduction of nitroarenes. Anilines can be oxidized using the heterogeneous catalysts and oxidants to produce azoxybenzenes [9–11]. However, this procedure provides the products with low selectivity and by-products in a large amount. On the other hand, nitroarenes can be reduced by using several types of methods [12–18]. But because of the complexity of multiple reduction steps, producing the highly selective azoxybenzenes often requires unique catalysts or complex reduction systems [19]. As well, azoxyarenes can be prepared from nitrosohydroxylamine ammonium salts [20], hydroxylamines [21], nitroso [22, 23] and azo compounds [24, 25]. As outlined in Scheme 1, types of intermediates and products are obtained during the reduction of nitroarenes. Accordingly, the use of appropriate reaction conditions is required to acquire a selective intermediate or product.

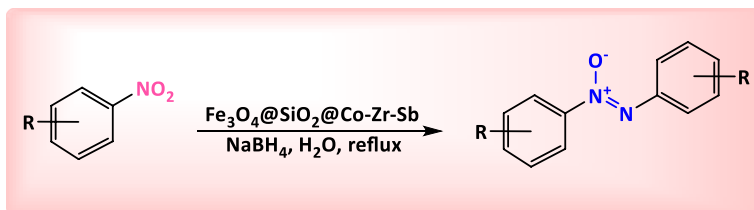
Currently, heterogeneous catalysts have been developed as a major part in various organic syntheses to improve and facilitate diverse synthetic reactions [26–40]. To date, the utilization of magnetic nanoparticles (MNPs) has attracted a lot of attention due to their easy separation by using an external magnetic field instead of usual filtration methods [41, 42]. Also, the application of magnetite core-shell nanocomposites as effective catalysts has been widely considered [43–52].

In addition, the use of trimetallic catalysts has been considerably attracted due to the better technological and scientific properties of this type of nanoparticles. The trimetallic NPs have been synthesized by various methods such as selective catalytic reduction, microwave, micro-emulsion, hydrothermal and co-precipitation. The surface of trimetallic nanoparticles is relatively unstable, so it easily precipitates from their solution and eventually reduces their catalytic activity. Thus, the trimetallic nanocomposites can be stabilized and synthesized with organic and inorganic compounds [53].

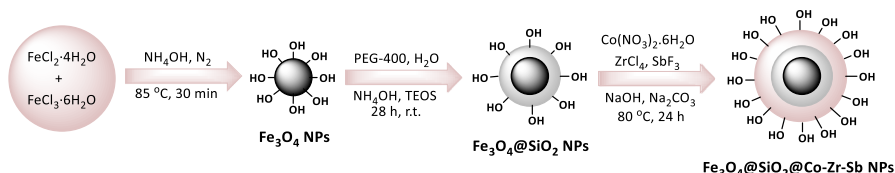
In recent years, the development of simple approaches for the synthesis of different chemical compounds, especially natural products and fundamental materials



Scheme 1 Reaction pathways during the reduction of nitroarenes



Scheme 2 One-pot reduction of nitroarenes to azoxyarenes with $\text{Fe}_3\text{O}_4@\text{SiO}_2@\text{Co-Zr-Sb}/\text{NaBH}_4/\text{H}_2\text{O}$ system



Scheme 3 Synthesis of nanomagnetic $\text{Fe}_3\text{O}_4@\text{SiO}_2@\text{Co-Zr-Sb}$ NPs

under green conditions, is desirable. In this regard, the use of heterogeneous magnetic trimetallic nanocomposites based on green chemistry under mild reaction conditions is required for efficient synthesis of azoxybenzenes.

In continuation of our research on the successful synthesis of layered double hydroxides (LDHs) with a combination of three cations on the surface of nanomagnetic cores [40], herein, we would like to report the novel recoverable trimetallic $\text{Fe}_3\text{O}_4@\text{SiO}_2@\text{Co-Zr-Sb}$ nanocatalyst for the chemoselective reduction of nitroarenes to azoxyarenes in the presence of NaBH_4 as a hydrogen donor in water, with a simple and by-product free approach (Scheme 2).

Results and discussion

Synthesis and characterizations of $\text{Fe}_3\text{O}_4@\text{SiO}_2@\text{Co-Zr-Sb}$ NPs

The magnetic nanocatalyst was prepared with an easy co-precipitation method using a three-step process: (i) preparation of magnetite NPs; (ii) synthesis of $\text{Fe}_3\text{O}_4@\text{SiO}_2$ NPs at ambient temperature; and (iii) growth of Co-Zr-Sb trimetallic nanoparticles on the surface of SiO_2 -layered Fe_3O_4 by an in situ growth method via aqueous solutions of Co^{2+} , Zr^{4+} and Sb^{3+} salts (Scheme 3). Also, $\text{Fe}_3\text{O}_4@\text{SiO}_2@\text{Co-Zr-Sb}$ nanocatalyst was characterized using various methods such as Fourier transform infrared (FT-IR) spectroscopy, scanning electron microscopy (SEM), energy-dispersive X-ray (EDX), vibrating sample magnetometer (VSM), transmission electron microscopy (TEM) and X-ray diffraction (XRD).

Firstly, the functional groups in the magnetic nanoparticles of Fe_3O_4 , $\text{Fe}_3\text{O}_4@\text{SiO}_2$ and $\text{Fe}_3\text{O}_4@\text{SiO}_2@\text{Co-Zr-Sb}$ were identified by the Fourier transform infrared spectroscopy. The strong absorption peak at low wavenumber (579 cm^{-1})

in the FT-IR spectrum of magnetite (Fig. 1a) comes from the vibration of Fe–O bonds in iron oxide. The absorption bands at around 3400 and 1625 cm^{-1} correspond to the O–H stretching and deforming modes in the adsorbed water, respectively. FT-IR spectrum of silica-layered magnetite (Fig. 1b) shows additional peaks compared to the Fe_3O_4 one. The broad bands at 1090 and 791 cm^{-1} are referred to the asymmetrical and symmetrical stretching vibrations of Si–O–Si, which confirm the presence of SiO_2 layers in the magnetic nanoparticles. Figure 1c exhibits the FT-IR spectrum of $\text{Fe}_3\text{O}_4@\text{SiO}_2@\text{Co-Zr-Sb}$ MNPs. The characteristic peaks of 3500 cm^{-1} (stretching band of metal hydroxyl groups and hydrogen-bonded water molecules), 1600 cm^{-1} (deformation absorption of water), 1385 cm^{-1} (stretching of interlayer CO_3^{2-} ions) and 500–1000 cm^{-1} (lattice vibration peaks of M–OH and M–O) indicate the structure in the core–shell nanocomposite.

The scanning electron microscopy (SEM) provides more detailed information on the morphology of the surface and size distribution of the synthesized magnetic nanomaterials (Fig. 2). The Fe_3O_4 nanoparticles show roughly granular and spherical shape in the range of 23–43 nm (Fig. 2a). As well, the microscopy image of $\text{Fe}_3\text{O}_4@\text{SiO}_2$ NPs represents uniform particles in the range of 22–30 nm (Fig. 2b). In the case of $\text{Fe}_3\text{O}_4@\text{SiO}_2@\text{Co-Zr-Sb}$ NPs with different magnifications, SEM images indicate that the surface of nanoparticles is modified and the size distribution is about 18–23 nm (Fig. 2c,d). Accordingly, the structure of nanocatalyst can be identified by SEM images.

The energy-dispersive X-ray spectroscopy is a convenient method for detecting elements with weight and atomic percentage in a material. EDX analysis of $\text{Fe}_3\text{O}_4@\text{SiO}_2@\text{Co-Zr-Sb}$ (Fig. 3) shows the presence of O, Si, Fe, Co, Zr and Sb elements in the structure of magnetic nanocomposite. This technique clearly

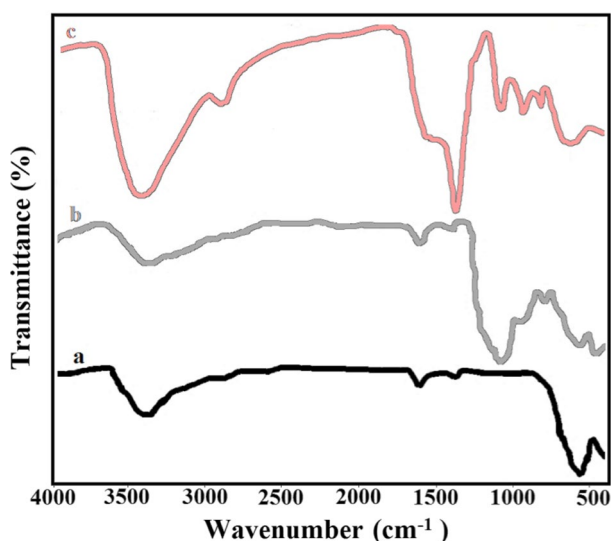


Fig. 1 FT-IR spectrum of **a** Fe_3O_4 , **b** $\text{Fe}_3\text{O}_4@\text{SiO}_2$, and **c** $\text{Fe}_3\text{O}_4@\text{SiO}_2@\text{Co-Zr-Sb}$ NPs

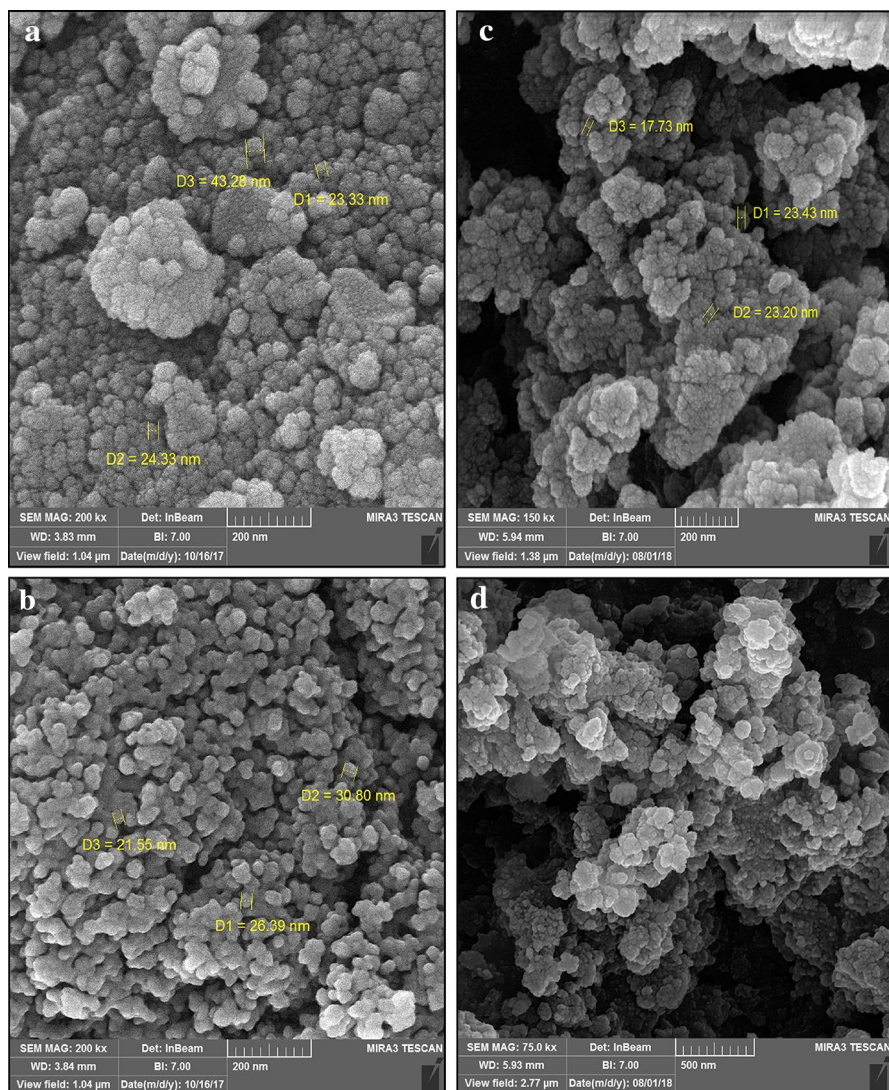


Fig. 2 SEM images of **a** Fe_3O_4 , **b** $\text{Fe}_3\text{O}_4@SiO_2$, and **c, d** $\text{Fe}_3\text{O}_4@SiO_2@Co-Zr-Sb$ NPs

shows that Co-Zr-Sb species have been successfully immobilized on the surface of $\text{Fe}_3\text{O}_4@SiO_2$ NPs.

Magnetic properties were studied by the vibrating sample magnetometer (VSM). Figure 4 illustrates the magnetic characterization of the synthesized samples. The curves clearly show a decrease in the amount of magnetism during the immobilization of a layer around the other. The saturation magnetization (M_s) value of Fe_3O_4 (Fig. 4a), $\text{Fe}_3\text{O}_4@SiO_2$ (Fig. 4b) and $\text{Fe}_3\text{O}_4@SiO_2@Co-Zr-Sb$

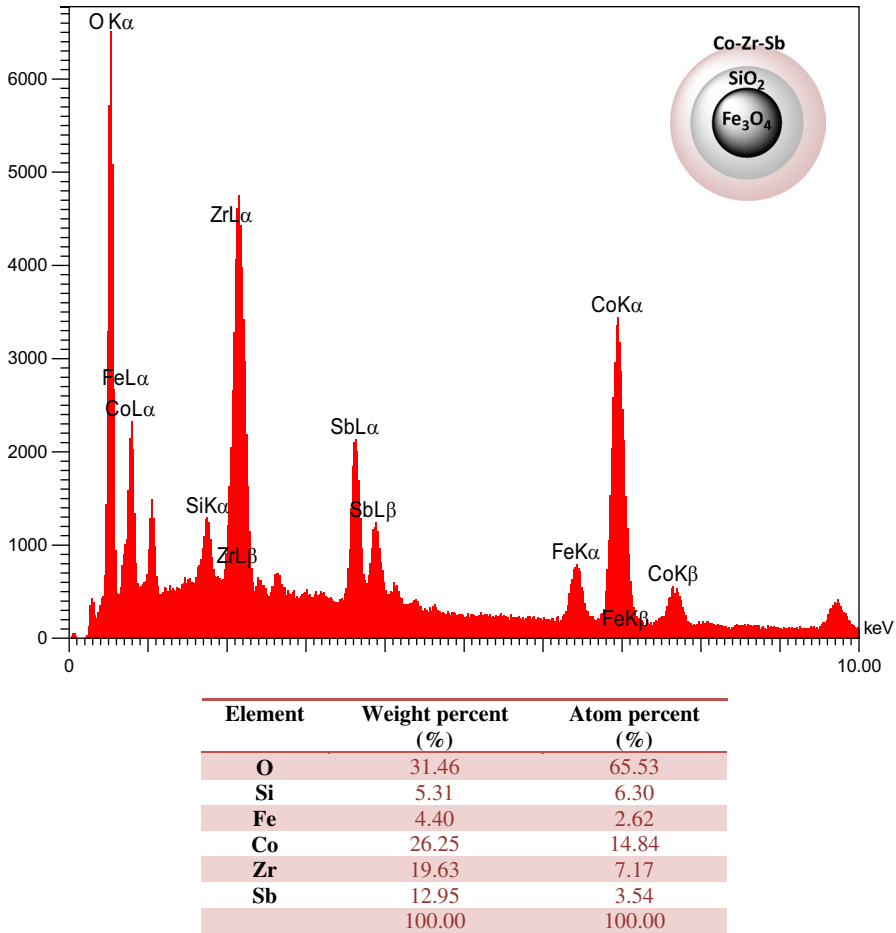


Fig. 3 EDX spectrum and elemental composition of $\text{Fe}_3\text{O}_4@\text{SiO}_2@\text{Co-Zr-Sb}$ NPs

NPs (Fig. 4c) is around 70, 30 and 4 emu g^{-1} , respectively. Therefore, the amount of Ms is reduced by coating one layer on another.

The transmission electron microscopy (TEM) provides more detailed information on the particle morphology of the as-prepared nanocomposite. TEM images of $\text{Fe}_3\text{O}_4@\text{SiO}_2@\text{Co-Zr-Sb}$ NPs indicate the dark cores surrounded by the other shells (Fig. 5).

The XRD pattern of Fe_3O_4 , $\text{Fe}_3\text{O}_4@\text{SiO}_2$ and $\text{Fe}_3\text{O}_4@\text{SiO}_2@\text{Co-Zr-Sb}$ NPs was measured by the X-ray diffraction (Fig. 6). Figure 6a represents the diffraction peaks at 2θ values of 30.2° , 35.5° , 43.3° , 53.7° , 57.2° and 62.9° correspond to (022), (113), (004), (224), (115) and (044) crystal planes of nanomagnetite. Fe_3O_4 has crystalline cubic spinel structure which agrees with the standard Fe_3O_4 XRD spectrum (JCPDS No. 65-3107). The same patterns of characteristic peaks were observed for $\text{Fe}_3\text{O}_4@\text{SiO}_2$ NPs (Fig. 6b), demonstrating that the embedded magnetite cores keep their

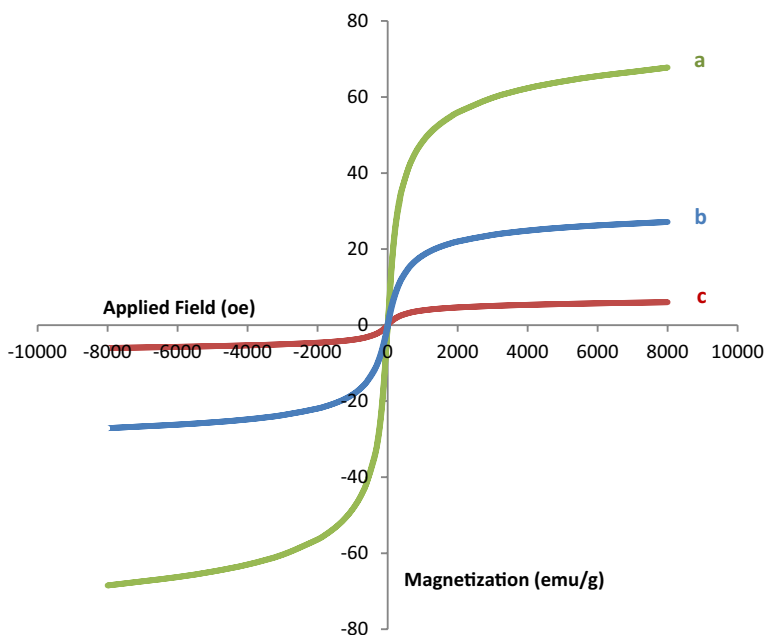


Fig. 4 Magnetization curve of (a) Fe_3O_4 , (b) $\text{Fe}_3\text{O}_4@ \text{SiO}_2$ and (c) $\text{Fe}_3\text{O}_4@ \text{SiO}_2@ \text{Co-Zr-Sb}$ NPs

crystalline phase after SiO_2 covering. Finally, the XRD pattern of $\text{Fe}_3\text{O}_4@ \text{SiO}_2@ \text{Co-Zr-Sb}$ (Fig. 6c,d) was investigated to determine the crystal structure. The X-ray diffraction pattern showed amorphous states and phases. To be sure, the XRD was repeated by another device and the results were the same. Accordingly, the synthesized nanocomposite has an amorphous structure.

Reductive coupling of nitroarenes to azoxyarenes

Initially, the trimetallic nanocomposite was prepared according to our previous research on the successful synthesis of LDHs with a combination of three cations on the surface of nanomagnetic cores. The main reason of choosing these metals is to provide three efficient cations for the synthesis of LDH-like nanocomposites and to observe their catalytic activity in various organic reactions. Due to this, the novel nanomagnetic $\text{Fe}_3\text{O}_4@ \text{SiO}_2@ \text{Co-Zr-Sb}$ catalyst has been successfully synthesized and characterized. The catalytic activity of prepared core-shell nanoparticles was investigated by the reductive coupling of nitrobenzenes to azoxybenzenes. This research was started with the primary aim of using the nanocatalyst to reduce nitroarenes to the corresponding anilines with sodium borohydride. Therefore, the reduction of nitrobenzene with reducing agent was selected as a model reaction in the presence of different catalytic amounts of nanocatalyst. At first, it was amazing to get orange red solution instead of aniline as an expected product. During further studies, the instrumental analysis confirmed the formation of azoxybenzene as a single product. The summarized results in Table 1 show the effect of some

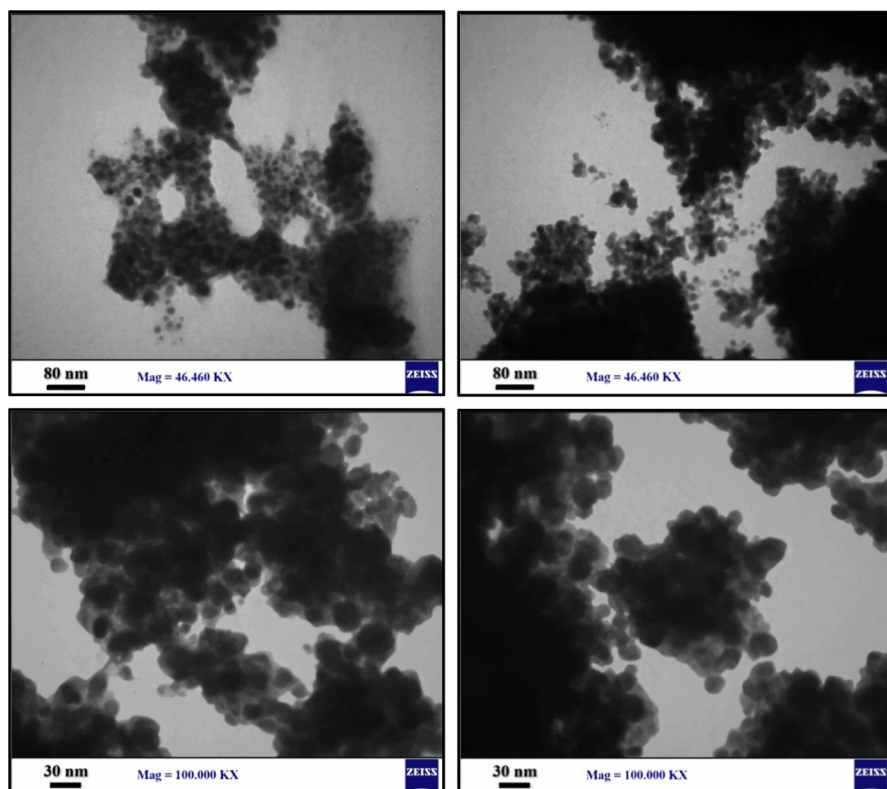


Fig. 5 TEM images of nanomagnetic- $\text{Fe}_3\text{O}_4@ \text{SiO}_2@ \text{Co-Zr-Sb}$ NPs

parameters on the model reaction. In the absence of the catalyst, the reaction showed no improvement. In order to study the effect of solvent, the model reaction is carried out in various solvents in the presence of heterogeneous nanocatalyst. Investigations revealed the optimal conditions for the synthesis of azoxybenzene. The starting compound was completely consumed using $\text{NaBH}_4/\text{H}_2\text{O}$ system under reflux conditions in the presence of the $\text{Fe}_3\text{O}_4@ \text{SiO}_2@ \text{Co-Zr-Sb}$ MNPs (Table 1, entry 11). The examinations exhibited that using nitrobenzene (1 mmol), $\text{Fe}_3\text{O}_4@ \text{SiO}_2@ \text{Co-Zr-Sb}$ MNPs (20 mg) and NaBH_4 (2 mmol) in refluxing water as a green solvent performs azoxybenzene within 3 min in 93% yield (Table 2, entry 1).

In the next step, the usability and generality of this study were investigated by the reduction of structurally diverse nitroarenes under optimized reaction conditions. The results show that in all cases, reductive coupling of nitroarenes occurred and the corresponding products were obtained in high yields (Table 2). The examinations revealed that nitroaromatic compounds (1 mmol) can be reduced using NaBH_4 (2 mmol) and $\text{Fe}_3\text{O}_4@ \text{SiO}_2@ \text{Co-Zr-Sb}$ MNPs (20 mg) in refluxing water within 2–10 min to provide azoxybenzenes in 83–93% yields.

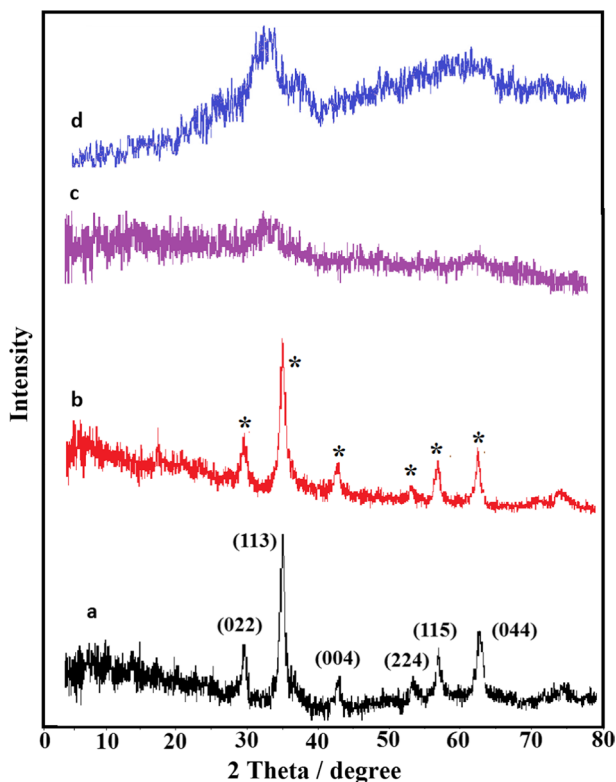
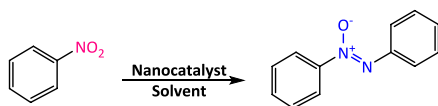


Fig. 6 XRD patterns of (a) Fe_3O_4 , (b) $\text{Fe}_3\text{O}_4@ \text{SiO}_2$ and (c), (d) $\text{Fe}_3\text{O}_4@ \text{SiO}_2@ \text{Co-Zr-Sb}$

The series of control experiments on the model reaction were investigated with Fe_3O_4 , SiO_2 , Co-Zr-Sb , $\text{Fe}_3\text{O}_4@ \text{SiO}_2$ and $\text{SiO}_2@ \text{Co-Zr-Sb}$ to illustrate that which part is the main catalytic site. The results revealed that the Co-Zr-Sb NPs immobilized on silica-layered magnetite is the most efficient catalyst and the other parts can react in longer time than the original reaction and of course the synthesis of azoxybenzenes cannot progress as well as the reported catalyst.

In addition, the synthesis of magnetic trimetallic catalyst was performed using the co-precipitation method. The molar ratios of Co/Zr/Sb were suggested in accordance with the proposed procedures for the synthesis of layered double hydroxides (LDHs) [32, 38]. Due to our experience with LDHs, we selected the appropriate molar ratio of cations in the catalyst formation. The synthesized nanocatalyst has three layers, each layer is coated on the other, and the analysis techniques can confirm this.

In order to study the suitability of this approach, the reductive coupling of nitrobenzene to azoxybenzene by $\text{NaBH}_4/\text{Fe}_3\text{O}_4@ \text{SiO}_2@ \text{Co-Zr-Sb}$ MNPs system was compared with previously reported methods (Table 3). The current investigation shows advantages in terms of recoverability and reusability of the

Table 1 Optimization experiments for reductive coupling of nitrobenzene to azoxybenzene with $\text{NaBH}_4/\text{Fe}_3\text{O}_4@\text{SiO}_2@\text{Co-Zr-Sb}$ NPs system under different reaction conditions

Entry	NaBH_4 (mmol)	Catalyst (g)	Solvent	Condition	Time (min)	Conversion (%)
1	2	–	H_2O	60–70 °C	300	–
2	2	0.02	H_2O	r.t.	90	Trace
3	–	0.02	H_2O	Reflux	180	0
4	2	0.02	H_2O	50–60 °C	90	20
5	2	0.02	H_2O	70–80 °C	40	95
6	2	0.02	EtOH	70–80 °C	40	70
7	2	0.02	$\text{EtOH}/\text{H}_2\text{O}$	70–80 °C	40	40
8	2	0.02	MeOH	70–80 °C	40	50
9	2	0.02	CH_3CN	70–80 °C	40	0
10	2	0.02	DMF	70–80 °C	40	Trace
11	2	0.02	H_2O	Reflux	3	100
12	2	0.01	H_2O	Reflux	7	100
13	2	0.03	H_2O	Reflux	2	100

All reactions were carried out with 1 mmol of nitrobenzene in 2 mL of solvent

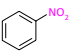
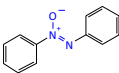
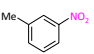
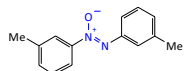
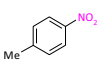
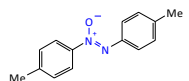
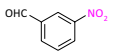
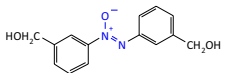
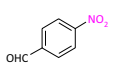
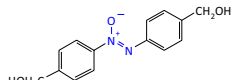
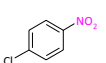
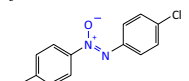
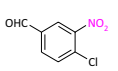
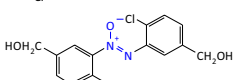
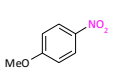
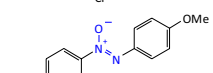
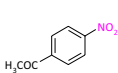
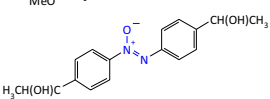
nanocatalyst, green reaction conditions, selective product formation, high yields and short reaction times.

Although the exact mechanism of this synthetic method is unclear, we propose the following plausible pathway for the one-pot reductive coupling of nitroarenes (Scheme 4). Reduction of nitrobenzenes to nitrosobenzenes (1) and phenylhydroxylamines (2) was taken place by the absorption of hydrogen on the surface of nanocatalyst, selectively. In the next step and through the activation of intermediates, the condensation of nitrosoarenes and arylhydroxylamines produced the corresponding azoxybenzenes with water loss.

Recycling of $\text{Fe}_3\text{O}_4@\text{SiO}_2@\text{Co-Zr-Sb}$ catalyst

The economic and green aspect of this procedure was examined by the reusability of $\text{Fe}_3\text{O}_4@\text{SiO}_2@\text{Co-Zr-Sb}$ MNPs in reductive coupling of nitroarene to azoxyarene under the optimized reaction conditions (Table 1, entry 11). After completion of the reaction, the nanocatalyst was magnetically separated from the reaction mixture, washed with EtOAc and then dried to use in the next runs. The catalyst can be reused for four consecutive cycles without the remarkable loss of catalytic activity (Fig. 7).

Table 2 Chemoselective hydrogenation of nitroarenes with $\text{NaBH}_4/\text{Fe}_3\text{O}_4@\text{SiO}_2@\text{Co-Zr-Sb}/\text{H}_2\text{O}$ system

Entry	Substrate	Product	Molar ratio Subs./ NaBH_4	Time (min)	Yield ^a (%)	M.p. (°C) (lit.)	References
1			1:2	3	93	< 35 (< 35)	[22]
2			1:2	8	87	< 35 (16)	[14]
3			1:2	6	90	67–69 (69)	[3]
4			1:3	5	83	109–111	–
5			1:3	2	85	193–195	–
6			1:2	4	88	97–99 (81–83)	[14]
7			1:3	5	83	147–149	–
8			1:2	6	91	113–115 (118, 135)	[3]
9			1:3	10	87	105–107	–

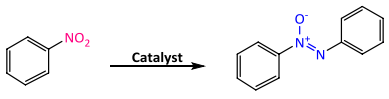
All reactions were carried out with $\text{Fe}_3\text{O}_4@\text{SiO}_2@\text{Co-Zr-Sb}$ (20 mg) and H_2O (2 mL) under reflux conditions

^aYields refer to isolated pure products

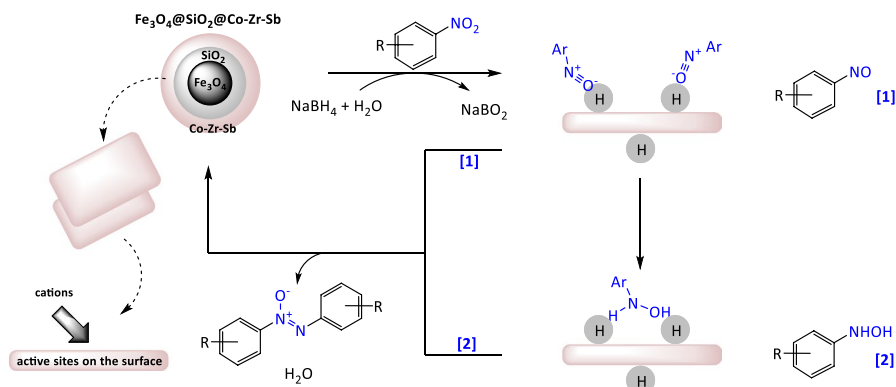
In addition, to study the reusability and durability of $\text{Fe}_3\text{O}_4@\text{SiO}_2@\text{Co-Zr-Sb}$ MNPs, FT-IR spectrum (Fig. 8) and SEM image (Fig. 9) of the recycled nanomagnetic catalyst was investigated. The results revealed that the structure of nanocatalyst is almost constant.

Experimental section

All chemical substrates were purchased from chemical companies and were used without further purification. ^1H NMR spectrum was measured by Bruker Avance spectrometer (300 MHz), and FT-IR spectra were obtained by Thermo Nicolet Nexus 670 apparatus. Mass spectra of the samples were obtained by mass spectrometer (Agilent, 5973 N, 20–70 eV). Morphology and size distribution of the

Table 3 Comparison of the current protocol for the reductive coupling of nitrobenzene to azoxybenzene with other reported systems


Entry	Catalyst system	Condition	Time (h)	Yield (%)	Reusability	References
1	NaBH ₄ /Fe ₃ O ₄ @SiO ₂ @Co-Zr-Sb	H ₂ O/reflux	0.05	93	4	^a
2	NaN(SiMe ₃) ₂	THF/150 °C	12	21	—	[18]
3	InBr ₃ /Et ₃ SiH	THF/60 °C	8	96	—	[19]
4	KBH ₄ /PEG-400	KOH/H ₂ O/reflux	4	61	—	[14]
5	NaBH ₄	Diglyme/90–100 °C/reflux	6	55	—	[13]
6	CuI/Ligand	NaOH/DMSO/H ₂ O/80 °C	8	85	—	[51]
7	Ru/C	EtOH/NaOH/THF/60 °C	18	89	—	[52]

^aPresent work**Scheme 4** A plausible mechanism for reductive coupling of nitrobenzenes to azoxybenzenes

particles were examined by SEM using FESEM-TESCAN and FESEM-ZEISS. Elemental composition of the sample was determined using EDX analysis. Magnetic properties of nanoparticles were measured by a vibration sample magnetometer (VSM, model MDKFT). TEM images were captured on a microscope (Zeiss EM10C) at accelerating voltage of 100 kV. The crystalline structure of the nanocatalyst was surveyed by X-ray diffraction on a Philips PANalytical X'Pert Pro diffractometer in a range of Bragg's angle ($2\theta = 5^\circ - 80^\circ$). TLC was utilized for reaction monitoring over silica gel 60 F₂₅₄ aluminum sheet.

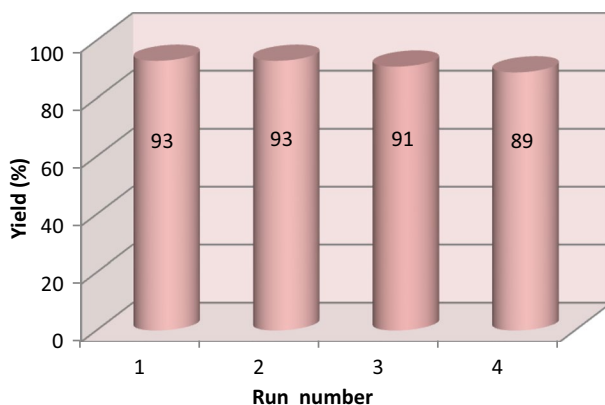


Fig. 7 Recycling of nanomagnetic- $\text{Fe}_3\text{O}_4@\text{SiO}_2@\text{Co-Zr-Sb}$ NPs in chemoselective hydrogenation of nitrobenzene

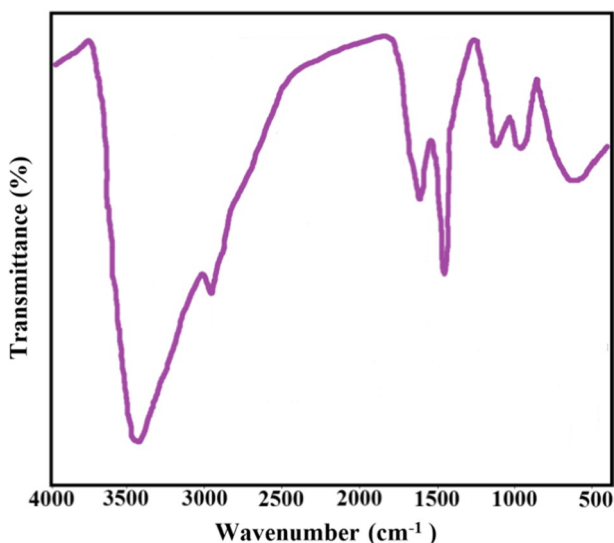


Fig. 8 FT-IR spectrum of nanomagnetic- $\text{Fe}_3\text{O}_4@\text{SiO}_2@\text{Co-Zr-Sb}$ after the second recovery

Synthesis of Fe_3O_4 NPs

Magnetite nanoparticles were synthesized by a chemical co-precipitation of chloride salts [54]. Commonly, a solution of 2.147 g of $\text{FeCl}_2 \cdot 4\text{H}_2\text{O}$ (0.0108 mol) and 5.838 g of $\text{FeCl}_3 \cdot 6\text{H}_2\text{O}$ (0.0216 mol) was prepared in H_2O (100 mL). The solution was stirred at 85 °C under N_2 atmosphere for 10 min. Next, by the addition of aqueous ammonia (25 wt%, 10 mL), the nanoparticles of Fe_3O_4 were immediately precipitated. The resulting mixture was stirred at 85 °C under N_2 atmosphere for 30 min. The mixture was cooled to the ambient temperature and nanoparticles of

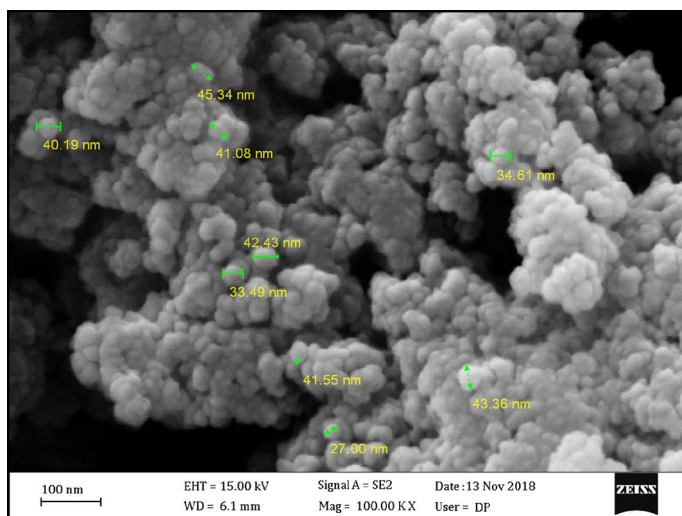


Fig. 9 SEM image of nanomagnetic- $\text{Fe}_3\text{O}_4@\text{SiO}_2@\text{Co-Zr-Sb}$ after the second recovery

Fe_3O_4 were magnetically separated. Magnetite was washed twice with a solution of NaCl and H_2O .

Synthesis of $\text{Fe}_3\text{O}_4@\text{SiO}_2$ NPs

SiO_2 layer was covered on the surface of Fe_3O_4 core according to the reported method [55]. Magnetite (1.5 g) was dispersed in water (20 mL); the suspension was added to 2-propanol (200 mL) and then homogenized by ultrasonic for 30 min. Under continuous stirring, polyethylene glycol-400 (5.36 g), H_2O (20 mL), aqueous ammonia (28 wt%, 10 mL) and tetraethyl orthosilicate (2 mL) were added sequentially into the suspension. The mixture was stirred for 28 h at ambient temperature. After completion of reaction, the product was magnetically separated and washed with H_2O and EtOH .

Synthesis of immobilized Co-Zr-Sb NPs on silica-coated magnetite ($\text{Fe}_3\text{O}_4@\text{SiO}_2@\text{Co-Zr-Sb}$ NPs)

Co-Zr-Sb trimetallic nanoparticles immobilized on SiO_2 -layered Fe_3O_4 have been prepared by the in situ growth method. Typically, 0.160 g of sodium hydroxide (0.004 mol), 1.060 g of sodium carbonate (0.01 mol) and 0.25 g of $\text{Fe}_3\text{O}_4@\text{SiO}_2$ were dispersed in 40 mL of H_2O . Another solution of $\text{Co}(\text{NO}_3)_2 \cdot 6\text{H}_2\text{O}$ (4.365 g, 0.015 mol), ZrCl_4 (0.349 g, 0.0015 mol) and SbF_3 (0.625 g, 0.0035 mol) in 40 mL of H_2O was prepared. Both of suspensions and solutions were sonicated for 60 min. Then, in a mean time and drop-wisely, they were added to a round-bottomed flask containing magnetic stirrer and water (40 mL). The resulting slurry was stirred for further 30 min at ambient temperature and subsequently was stored for 24 h at

80 °C. The mixture was cooled to the ambient temperature and then filtered. Next, the product was dried at 50 °C to afford $\text{Fe}_3\text{O}_4@\text{SiO}_2@\text{Co-Zr-Sb}$ MNPs as a solid material in 3.15 g.

A typical procedure for the chemoselective hydrogenation of nitrobenzene

A mixture of 20 mg of $\text{Fe}_3\text{O}_4@\text{SiO}_2@\text{Co-Zr-Sb}$ MNPs and 0.123 g of nitrobenzene (1 mmol) in 2 mL of water was stirred for a minute. Next, NaBH_4 (0.076 g, 2 mmol) was added and the mixture was stirred under reflux conditions for 3 min. The formation of azoxybenzene was determined by changing the color of the mixture to orange red. TLC indicated the progress of reaction ($\text{EtOAc}/n\text{-hexane}$: 2/5). Next, the mixture was cooled to the room temperature. The nanocatalyst was magnetically separated, and the reaction mixture was then extracted with ethyl acetate (2×5 mL). The combined organic layers were dried over anhydrous sodium sulfate. Evaporation of solvent provided pure azoxybenzene in 93% yield (Table 2, entry 1).

Conclusions

In conclusion, the novel efficient $\text{Fe}_3\text{O}_4@\text{SiO}_2@\text{Co-Zr-Sb}$ catalyst has been developed for the chemoselective hydrogenation of nitroarenes to azoxyarenes under green conditions using NaBH_4 as a hydrogen donor. The recoverable heterogeneous nanocatalyst has been characterized using FT-IR, SEM, EDX, VSM, TEM and XRD analyses. Reductive coupling of nitrobenzenes was carried out successfully within 2–10 min to give products in good to high yields. Undoubtedly, this practical approach can open a new way for proper and green reduction of nitroarenes to azoxyarenes. This synthetic procedure offers several advantages in terms of mild reaction conditions, short reaction times, absence of hazardous organic solvents, using water as a green solvent and reusability of the magnetic nanocatalyst.

Acknowledgements The authors gratefully acknowledge the financial support of this work by the research council of Urmia University.

References

1. M.I. Qadir, J.D. Scholten, J. Dupont, *Catal. Sci. Technol.* **5**, 1459 (2015)
2. Y.F. Chen, J. Chen, L.J. Lin, G.J. Chuang, *J. Org. Chem.* **82**, 11626 (2017)
3. A. Rezaeifard, M. Jafarpour, M.A. Naseri, R. Shariati, *Dyes Pigments* **76**, 840 (2008)
4. J.M. Huang, J.F. Kuo, C.Y. Chen, *J. Appl. Polym. Sci.* **55**, 1217 (1995)
5. D. Campbell, L.R. Dix, P. Rostron, *Dyes Pigments* **29**, 77 (1995)
6. M. Gamberini, M.R. Cidade, L.A. Valotta, M.C. Armelin, L.C. Leite, *Carcinogenesis* **19**, 147 (1998)
7. A.B.E. Vix, P. Muller-Buschbaum, W. Stocker, M. Stamm, J.P. Rabe, *Langmuir* **16**, 10456 (2000)
8. C.L. Folcia, I. Alonso, J. Ortega, J. Etxebarría, I. Pintre, M.B. Ros, *Chem. Mater.* **18**, 4617 (2006)
9. S. Ghosh, S.S. Acharyya, T. Sasaki, R. Bal, *Green Chem.* **17**, 1867 (2015)
10. S.S. Acharyya, S. Ghosh, R. Bal, *ACS Sustain. Chem. Eng.* **2**, 584 (2014)
11. C.F. Chang, S.T. Liu, *J. Mol. Catal. A: Chem.* **299**, 121 (2009)
12. H.J. Shine, H.E. Mallory, *J. Org. Chem.* **27**, 2390 (1962)

13. C.E. Weill, G.S. Panson, *J. Org. Chem.* **21**, 803 (1956)
14. Y. Liu, B. Liu, A. Guo, Z. Dong, S. Jin, Y. Lu, *Molecules* **16**, 3563 (2011)
15. Z. Hou, Y. Fujiwara, H. Taniguchi, *J. Org. Chem.* **53**, 3118 (1988)
16. A. McKillop, R.A. Raphael, E.C. Taylor, *J. Org. Chem.* **35**, 1670 (1970)
17. Y. Lu, J. Liu, G. Diffée, D. Liu, B. Liu, *Tetrahedron Lett.* **47**, 4597 (2006)
18. J.R. Hwu, A.R. Das, C.W. Yang, J.J. Huang, M.H. Hsu, *Org. Lett.* **7**, 3211 (2005)
19. N. Sakai, K. Fujii, S. Nabeshima, R. Ikeda, T. Konakahara, *Chem. Commun.* **46**, 3173 (2010)
20. J.R. Hwu, C.S. Yau, S.C. Tsay, T.I. Ho, *Tetrahedron Lett.* **38**, 9001 (1997)
21. A.R. Becker, L.A. Sternson, *J. Org. Chem.* **45**, 1708 (1980)
22. B. Zhou, J. Song, T. Wu, H. Liu, C. Xie, G. Yang, B. Han, *Green Chem.* **18**, 3852 (2016)
23. J.A. Hrabie, L.K. Keefer, *Chem. Rev.* **102**, 1135 (2002)
24. M. Nakata, S. Kawazoe, T. Tamai, K. Tatsuta, H. Ishiwata, Y. Takahashi, Y. Okuno, T. Deushi, *Tetrahedron Lett.* **34**, 6095 (1993)
25. B.T. Newbold, *J. Org. Chem.* **27**, 3919 (1962)
26. M. Boudart, *Chem. Rev.* **95**, 661 (1995)
27. M. Heitbaum, F. Glorius, I. Escher, *Angew. Chem. Int. Ed.* **45**, 4732 (2006)
28. H. Hattori, *Chem. Rev.* **95**, 537 (1995)
29. N. Mizuno, M. Misono, *Chem. Rev.* **98**, 199 (1998)
30. M.R. Othman, Z. Helwani, Martunus, W.J.N. Fernando, *Appl. Organomet. Chem.* **23**, 335 (2009)
31. A. Corma, H. Garcia, F.X. Llabres i Xamena, *Chem. Rev.* **110**, 4606 (2010)
32. M. Gilanizadeh, B. Zeynizadeh, *New J. Chem.* **42**, 8553 (2018)
33. M. Gilanizadeh, B. Zeynizadeh, *Res. Chem. Intermed.* **44**, 6053 (2018)
34. A. Baghban, E. Doustkhah, S. Rostamnia, *Int. Nano Lett.* **8**, 41 (2018)
35. M. Gilanizadeh, B. Zeynizadeh, *J. Iran. Chem. Soc.* **15**, 2821 (2018)
36. B. Zeynizadeh, E. Gholamiyan, M. Gilanizadeh, *Curr. Chem. Lett.* **7**, 121 (2018)
37. M. Gilanizadeh, B. Zeynizadeh, E. Gholamiyan, *Iran. J. Sci. Technol. Trans. A: Sci.* **43**, 819 (2019)
38. B. Zeynizadeh, M. Gilanizadeh, *New J. Chem.* **43**, 18794 (2019)
39. M. Gilanizadeh, B. Zeynizadeh, *Polycycl. Aromat. Compd.* (2019). (in press)
40. M. Gilanizadeh, B. Zeynizadeh, *Res. Chem. Intermed.* **45**, 2811 (2019)
41. V. Polshettiwar, R. Luque, A. Fihri, H. Zhu, M. Bouhrara, J.M. Basset, *Chem. Rev.* **111**, 3036 (2011)
42. R.G. Chaudhuri, S. Paria, *Chem. Rev.* **112**, 2373 (2012)
43. F. Niu, L. Zhang, S.Z. Luo, W.G. Song, *Chem. Commun.* **46**, 1109 (2010)
44. R. Cano, D.J. Ramon, M.J. Yus, *Org. Chem.* **75**, 3458 (2010)
45. T. Poursaberi, V. Akbar, S.M.R. Shoja, *Iran. J. Chem. Chem. Eng.* **34**, 41 (2015)
46. M. Ma, J. Xie, Y. Zhang, Z. Chen, N. Gu, *Mater. Lett.* **105**, 36 (2013)
47. M. Kotani, T. Koike, K. Yamaguchi, N. Mizuno, *Green Chem.* **8**, 735 (2006)
48. K.V.S. Ranganath, J. Kloesges, A.H. Schafer, F. Glorius, *Angew. Chem. Int. Ed.* **49**, 7786 (2010)
49. H. Cai, K. Li, M. Shen, S. Wen, Y. Luo, C. Peng, G. Zhang, X. Shi, *J. Mater. Chem.* **22**, 15110 (2012)
50. B. Zeynizadeh, F. Faraji, *RSC Adv.* **9**, 13112 (2019)
51. Z. Chen, Y. Qiu, X. Wu, Y. Ni, L. Shen, J. Wu, S. Jiang, *Tetrahedron Lett.* **59**, 1382 (2018)
52. J.H. Kim, J.H. Park, Y.K. Chung, K.H. Park, *Adv. Synth. Catal.* **354**, 2412 (2012)
53. G. Sharma, D. Kumar, A. Kumar, A.H. Al-Muhtaseb, D. Pathania, M. Naushad, G.T. Mola, *Mater. Sci. Eng. C* **71**, 1216 (2017)
54. X. Liu, Z. Ma, J. Xing, H. Liu, *J. Magn. Magn. Mater.* **270**, 1 (2004)
55. Y. Zhang, G.M. Zeng, L. Tang, D.L. Huang, X.Y. Jiang, Y.N. Chen, *Biosens. Bioelectron.* **22**, 2121 (2007)